

Article

Modeling the Mechanical Properties of Heat-Treated Mg-Zn-RE-Zr-Ca-Sr Alloys with the Artificial Neural Network and the Regression Model

Yu Fu *, Zhiwen Shao, Chen Liu, Yinyang Wang, Yongdong Xu * and Xiurong Zhu

Ningbo Branch of China Academy of Ordnance Science, Ningbo 315103, China; lourry@163.com (Z.S.); chenliu52s@imr.ac.cn (C.L.); wangyinyang929@126.com (Y.W.); zxr0922@163.com (X.Z.)

* Correspondence: fuyuyayu@126.com (Y.F.); ydxu108@163.com (Y.X.);
Tel.: +86-574-87902206 (Y.F.); +86-574-87902206 (Y.X.)

Abstract: In this study, an artificial neural network approach and a regression model are adopted to predict the mechanical properties of heat-treated Mg-Zn-RE-Zr-Ca-Sr magnesium alloys. The dataset for artificial neural network (ANN) modeling is generated by investigating the microhardness of heat-treated Mg-Zn-RE-Zr-Ca-Sr alloys using Vickers hardness tests. A back-propagation (BP) neural network is established using experimental data that enable the prediction of mechanical properties as a function of the composition and heat treatment process. The input variables for the BP network model are Ca and Sr contents, ageing temperature and ageing time. The output variable corresponds to the microhardness. The optimal BP network model is acquired by optimizing the number of the hidden layer nodes. The results indicate that a reliable correlation coefficient is above 0.95 for architecture (4-8-1), which has a high level of accuracy for prediction. In addition, a second-order polynomial regression model is developed based on the least squares method. The results of determination coefficients and Fisher's criterion indicate that the regression model is capable of modeling mechanical properties as a function of composition and the ageing process. Furthermore, supplemental experiments are conducted to check the accuracy of the BP model and the regression model, suggesting that the model predictions are well in accordance with experimental results. Therefore, both the BP network and regression models have high accuracy in modeling and predicting mechanical properties of heat-treated Mg-Zn-RE-Zr-Ca-Sr alloys.

Keywords: artificial neural network; regression analysis; mechanical properties; ageing treatment; Mg-Zn-RE-Zr-Ca-Sr alloys



Citation: Fu, Y.; Shao, Z.; Liu, C.; Wang, Y.; Xu, Y.; Zhu, X. Modeling the Mechanical Properties of Heat-Treated Mg-Zn-RE-Zr-Ca-Sr Alloys with the Artificial Neural Network and the Regression Model. *Crystals* **2022**, *12*, 754. <https://doi.org/10.3390/cryst12060754>

Academic Editors: Alla S. Sologubenko and Mingyi Zheng

Received: 26 April 2022

Accepted: 22 May 2022

Published: 24 May 2022

Publisher's Note: MDPI stays neutral with regard to jurisdictional claims in published maps and institutional affiliations.



Copyright: © 2022 by the authors. Licensee MDPI, Basel, Switzerland. This article is an open access article distributed under the terms and conditions of the Creative Commons Attribution (CC BY) license (<https://creativecommons.org/licenses/by/4.0/>).

1. Introduction

With the emergence of environmental and energy issues, light-weight magnesium alloys have attracted more and more attention. Due to their high specific strength and stiffness, superb castability and outstanding recyclability, magnesium (Mg) alloys have been widely used in aerospace, automotive and electronic industries [1–3]. The mechanical properties of Mg alloys are affected by the concentration of alloying elements. In addition, the properties of Mg alloys are further improved by employing relevant heat treatment or other engineering processes [4]. Existing resources lack the ability to predict the properties from a given chemical composition and processing parameters. Prediction ability is essential in optimizing or tailoring Mg alloys and for fully utilizing an alloy's potential.

The ZE41 magnesium alloy is one of the most popular of the Mg-Zn-RE (rare earth)-Zr based alloys and has been widely used for aircraft gearboxes and generator housings on military helicopters [5–7]. Over the past few decades, many researchers have endeavored to study the strengthening mechanism, heat treatment technology and microstructure evolution of Mg-Zn-RE-Zr alloys [8–10]. The relationship between process parameters and mechanical properties for Mg-Zn-RE-Zr alloys has only been studied empirically. It

is difficult to use a single mathematical model to describe the relationship between heat treatment parameters and mechanical properties of Mg-Zn-RE-Zr alloys.

In recent years, artificial neural networks (ANNs) have become powerful and flexible modeling tools that can lead to significant improvements in materials science for modeling complex problems and exploring the correlations between processes and properties [11–14]. They are particularly suitable to treat phenomena that have multiple inputs and have complex nonlinear relationships between input and output values. Yang employed the ANN model with a back-propagation (BP) algorithm to explore the correlations between heat treatment processes and mechanical properties of A357 alloy [15]. Conduit developed an ANN to enable the prediction of an individual material's properties both as a function of the composition and heat treatment routine [16]. Furthermore, Malinov established an ANN model to analyze and predict the correlation between heat treatment parameters and mechanical properties in titanium alloys [17,18].

In addition, multiple regression analysis was applied to build the input–output relationship in many casting processes [19,20]. Multiple regression analysis generates curves that fit the discrete data obtained from experiments to allow estimates at intermediate points. Chen applied a nonlinear mathematical model to quantitatively analyze the effects of heat treatment on the Vickers hardness of an Al-Si-Mg alloy, obtaining the optimum heat treatment process by using the sequential approximation optimization method [21]. However, models for predicting mechanical properties of Mg-Zn-RE-Zr alloys have rarely been reported.

In this work, an ANN model and a multiple regression model were developed to predict the mechanical properties of heat-treated Mg-Zn-RE-Zr-Ca-Sr alloys. Figure 1 illustrates the flow diagram of the methodology used in this study. Firstly, a systematic experimental investigation of the effects of alloying elements and ageing treatment on the mechanical properties of Mg-Zn-RE-Zr-Ca-Sr alloys was carried out. Secondly, based on the experimental data, an ANN model and a regression model were developed to predict the mechanical properties of experimental alloys as a function of alloying elements and ageing process parameters. Finally, both the models were validated by the experiments. This work aims to provide a new strategy for the development of Mg alloys.

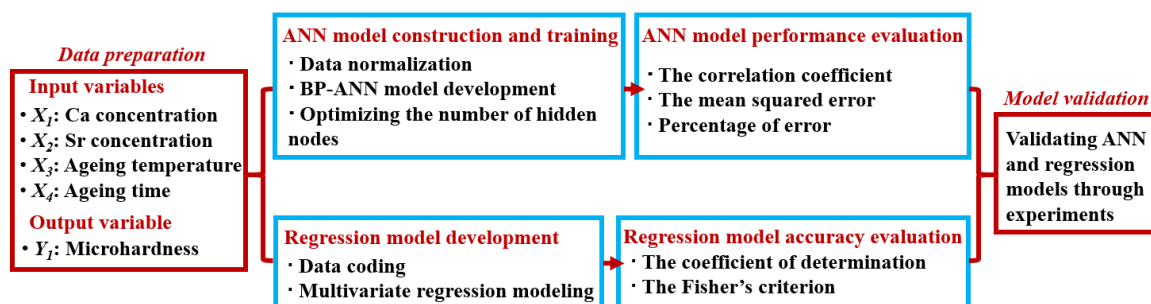


Figure 1. The flow chart of this study.

2. Experiments and Methods

2.1. Experimental Procedure

This study was conducted on the Mg-4.2Zn-1.7RE-0.8Zr- x Ca- y Sr ($x = 0, 0.2$ wt.%; $y = 0, 0.1, 0.2, 0.4$ wt.%) alloys due to their advantages such as excellent fluidity, good heat resistance and low wall thickness effect. The casting ingots were produced by Mg, Zn, Ce-rich mischmetal (50 wt.% Ce, 28 wt.% La, 16 wt.% Nd, 4% wt.% Pr and 2 wt.% impurity), Mg-30Zr, Mg-20Ca and Mg-20Sr in an electric resistance furnace under an argon atmosphere at 730 °C. Then, the samples were subjected to different heat treatments. The chemical compositions of the as-cast alloys were measured by the X-ray fluorescence (XRF) method and the results are presented in Table 1. Experiments were designed according to the underage, peak age and overage conditions. Therefore, the ageing temperature was set at 300 °C, 325 °C and 350 °C, and the ageing time ranged from 0 h to 32 h. After

ageing treatment, Vickers hardness tests were performed with a 1 kg load. Ten indentations per sample were analyzed to improve precision. The average value was reported as the microhardness (HV). Table A1 in Appendix A, which is attached to the end of this article, summarizes the experimental results.

Table 1. Chemical compositions of the as-cast alloys (wt.%).

	Nominal Alloys	Actual Composition					
		Mg	Zn	RE	Zr	Ca	Sr
1	Mg-4.2Zn-1.7RE-0.8Zr	Bal.	4.11	1.62	0.70	-	-
2	Mg-4.2Zn-1.7RE-0.8Zr-0.2Ca	Bal.	4.14	1.61	0.76	0.18	-
3	Mg-4.2Zn-1.7RE-0.8Zr-0.2Ca-0.1Sr	Bal.	4.03	1.67	0.67	0.19	0.11
4	Mg-4.2Zn-1.7RE-0.8Zr-0.2Ca-0.2Sr	Bal.	4.13	1.72	0.69	0.22	0.21
5	Mg-4.2Zn-1.7RE-0.8Zr-0.2Ca-0.4Sr	Bal.	4.11	1.64	0.75	0.17	0.38

2.2. BP Neural Network Modeling

An ANN is a mathematical model consisting of many highly interconnected processing elements organized into layers. The ANN keeps knowledge with connection weights [22]. Input–output pairs are presented to the ANN and the weights are adjusted to minimize the error between the predicted outputs and actual values. A multilayered neural network (MLP) is used to develop an ANN model which is used to predict the mechanical properties of the heat-treated Mg-Zn-RE-Zr-Ca-Sr alloys. Since the back-propagation (BP) algorithm is a representative method to reduce the errors created by the gradient descent method, it is used to train the multilayer feed forward network. A BP network model is developed using MATLAB R2018a[®]. The architecture of the BP neural network is presented in Figure 2, which includes the input layer (four neurons), one hidden layer and the output layer (one neuron). The input variables of the BP model contain the Ca content, Sr content, ageing temperature and ageing time. The output variable is microhardness.

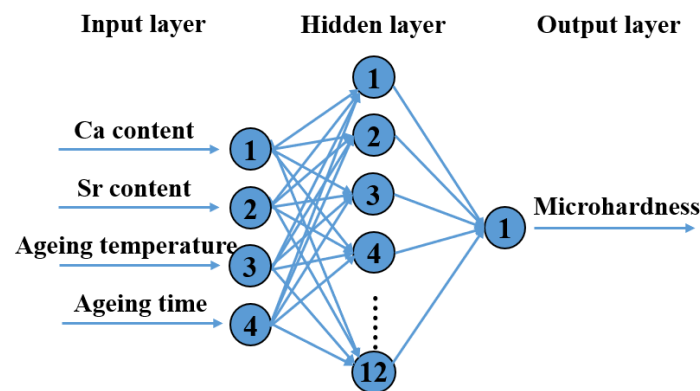


Figure 2. The architecture of the three-layered BP neural network in the present study.

It should provide a concise and precise The data for training, testing and validation were generated from 77 groups of experiments, as discussed in Section 2.1, which are shown in Table A1 in Appendix A. In order to avoid over fitting in the BP network training, 77 groups of data were randomly divided into three subsets: 70% training set, 15% test set and 15% validation set. Then, both inputs and outputs were fed into the neural network toolbox. The general procedure is described step by step as follows:

- (1) In order to decrease the order-of-magnitude difference in the various dimensions, the experimental dataset was normalized between -1 and 1 using the following formula:

$$X_N = 2 \left(\frac{X - X_{min}}{X_{max} - X_{min}} \right) - 1 \quad (1)$$

where X_N is the normalized value of a certain variable and X is the experimental value for this variable. Furthermore, X_{min} and X_{max} are the minimum and the maximum in the dataset for this variable, respectively.

- (2) Table 2 shows the architecture and training parameters of the BP neural network. The hyperbolic tangent ‘tan-sigmoid’ and linear transfer ‘Purelin’ functions were used as activation transfer functions. The mathematical model of the BP neural network is shown in Figure 3. Compared with the standard gradient descent algorithm, the Levenberg–Marquardt (LM) algorithm possesses fast convergence and a small mean square error [22]. As a result, the BP neural network was trained using the LM algorithm. To evaluate the performance of the developed BP network model, the correlation coefficient (R), the percentage of error and the mean squared error (MSE) were quantified as follows:

$$R = \frac{\sum_{i=1}^n (T_i - \bar{T})(Y_i - \bar{Y})}{\sqrt{\sum_{i=1}^n (T_i - \bar{T})^2 \sum_{i=1}^n (Y_i - \bar{Y})^2}} \tag{2}$$

$$\text{Percentage of error (\%)} = 100 \left(\frac{T_i - Y_i}{T_i} \right) \tag{3}$$

$$MSE = \frac{1}{n} \sum_{i=1}^n (T_i - Y_i)^2 \tag{4}$$

where T_i is the experimental value and Y_i is the predicted value. Furthermore, \bar{T} and \bar{Y} are the mean values of all the experimental and predicted results, respectively. n is the total number of data pairs in this investigation. The convergence of MSE to 0.005 was established in 1000 epochs.

- (3) The BP neural network was optimized by adjusting the number of hidden neurons. The effect of the number of hidden neurons on output variables was also studied. The number of hidden neurons was estimated according to the empirical equation:

$$M = \sqrt{n + m} + a \tag{5}$$

where m and n are the number of neurons in the input layer and output layer, respectively, and a is a constant ranging from 1 to 10 [23,24]. In order to obtain the optimal architecture, ten different BP network models were tested.

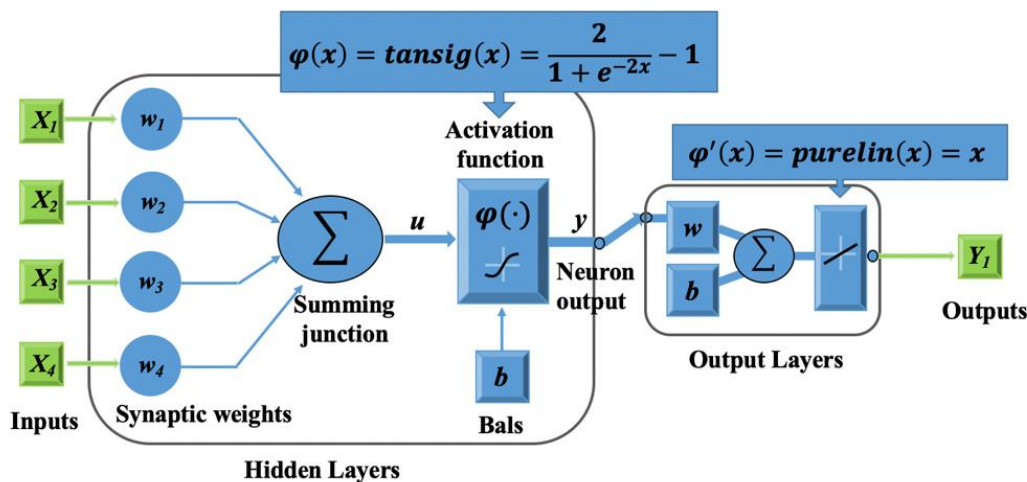


Figure 3. The mathematical model of the BP neural network.

Table 2. The architecture and training parameters of the BP neural network.

Parameters	BP Neural Network
Number of layers	3
Number of neurons on the layers	Input: 4, Hidden: 4~12, Output: 4
Transfer functions	Hidden layer: Tan-Sigmoid Output layer: Purelin
Train method	Levenberg–Marquardt (LM)
Initial weights and biases	Randomly between −1 and 1
Target error value	0.0167
Learning rate	Variable learning rate

2.3. Multiple Regression Modeling

The key to alloy prediction is knowing the relationships between chemical composition, processing parameters and mechanical properties. Much of this information is mainly divided into two categories: (1) relationships that are based on physical principles and reflect the essence of the process and physical and chemical interactions among the factors, and (2) relationships that are obtained by mathematical means that experimentally treat obtained data and manipulate these data to obtain relationships between the independent and dependent variables without emphasizing physical meanings. This method was adopted in this study. The second-order polynomial regression model was employed to build the multivariate regression model for microhardness. The input variables were coded based on the minimum and maximum. The corresponding equation is as follows:

$$x_i = 2 \left(\frac{X_i - X_{i0}}{\Delta X_i} \right) \quad (6)$$

where x_i ($i = 1, 2, 3, 4$) is the coded input variable and X_i is the actual input variable. X_{i0} is the value of X_i at the center level and ΔX_i is the variation range in X_i . The input variables and their levels are shown in Table 3.

Table 3. Input variables and their levels.

Levels	Input Variables			
	X_1 : Ca Content, wt.%	X_2 : Sr Content, wt.%	X_3 : Ageing Temperature, °C	X_4 : Ageing Time, h
Low level (−1)	0	0	300	0.125
Center level (0)	0.1	0.2	325	15.9375
High level (1)	0.2	0.4	350	32
Variation range (ΔX_i)	0.2	0.4	50	31.875

The second-order polynomial regression model describing HV is presented below:

$$HV(x) = b_0 + \sum_{i=1}^4 b_i x_i + \sum_{i=1}^4 \sum_{j=i+1}^4 b_{ij} x_i x_j + \sum_{i=1}^4 b_{ii} x_i^2 \quad (7)$$

where b_0 is a constant, and b_i , b_{ii} and b_{ij} ($i, j = 1, 2, 3, 4$) are the coefficients of the linear, quadratic and cross product terms, respectively. In addition, the coefficients were calculated using the least squares method, which is a trial-and-error process. The statistical accuracy of regression models was determined using the coefficient of determination (R^2) and the Fisher's criterion (F -test).

3. Results and Discussion

3.1. BP Neural Network Results

BP neural networks are developed based on trial and error by adjusting the number of neurons in the hidden layer. Figure 4 shows the correlation coefficient (R) values obtained

from the trained BP model for HV from different numbers of hidden neurons, suggesting an analysis of the network response in the form of a linear regression between the network outputs and corresponding targets for the dataset. The R values for all cases—training, validation and test—are nearly the same for all runs. An R near 1 suggests that a regression line fits the data well. Therefore, it is observed that the R value is above 0.95 for architecture (4-8-1) which has a high level of accuracy for prediction. Figure 5 shows the training error curve of the 4-8-1 BP neural network. It is found that the MSE decreases with an increasing number of iterations. The training process lasts until the error goal is close to 0.005. Each epoch is a step that passes through inputs, hidden layers and outputs in the training process of the BP neural network.

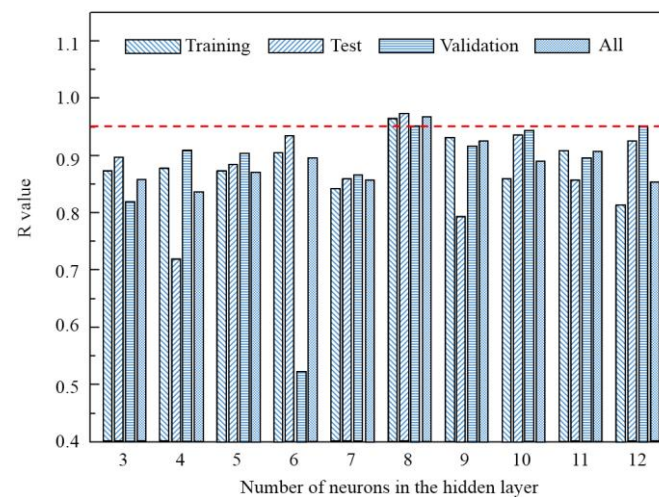


Figure 4. The correlation coefficient (R) values obtained from the trained BP model for HV from different numbers of hidden neurons.

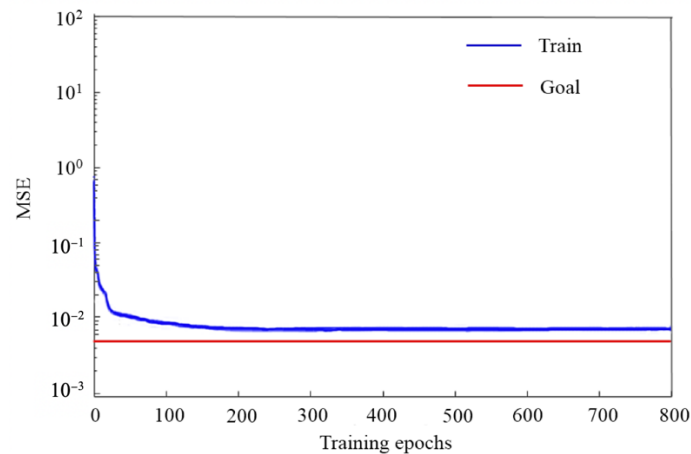


Figure 5. The training error curve of the 4-8-1 BP neural network.

The comparisons between the experimental and the predicted results for the entire dataset of 77 experiments are shown in Figure 6. The fitting line observed in Figure 6 indicates good agreement between the predicted and experimental values, and the adjust R square is found to be above 0.95. This suggests that there is a reliable correlation between alloying elements, ageing treatment parameters and microhardness of the Mg-4.2Zn-1.7RE-0.8Zr-xCa-ySr alloy. The result presented here gives confidence that the 4-8-1 BP network model can predict with sufficient accuracy.

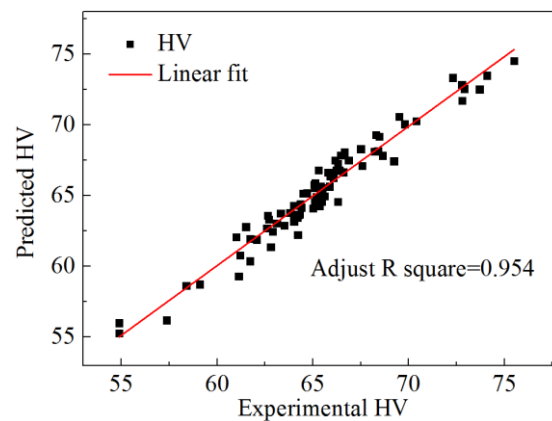


Figure 6. Analysis of the correlation coefficient between the experimental and predictive values.

Furthermore, the predictive ability of the 4-8-1 BP model is further tested by experiments. Table 4 presents the experimental data gained from Vickers hardness tests and corresponding BP results of simulating data. The average percentage error is less than $\pm 3\%$, which means the BP model's predicted results are close to the experimental results. Figure 7 presents the experimental versus BP-predicted results for HV, which reveal that the prediction of BP model is found to be in good agreement with the experimental data. Therefore, the BP neural network can be used to predict mechanical properties of heat-treated Mg-Zn-RE-Zr alloys processed within the inputs of Ca content, Sr content, ageing temperature and ageing time.

Table 4. Experimental data and BP predicted results.

No.	Ca Content, wt.%	Sr Content, wt.%	Ageing Temperature, °C	Ageing Time, h	Experimental HV	Predicted HV	Percentage of Error, %
1	0	0	300	0.25	57.8	57.08	1.17
2	0	0	300	4	66.6	67.79	-1.72
3	0	0	300	24	65.2	63.82	2.16
4	0	0	325	0.125	54.9	55.59	-1.29
5	0	0	325	12	66.1	67.97	-2.88
6	0	0	325	24	64.5	63.08	2.14
7	0	0	350	0.5	60.3	59.43	1.36
8	0	0	350	6	63.2	64.24	-1.62
9	0	0	350	16	62.9	64.75	-2.95
10	0.2	0	325	1	62.6	62.89	-0.55
11	0.2	0	325	6	67.8	66.98	1.21
12	0.2	0	325	12	74.3	75.19	-1.27
13	0.2	0	325	24	64.9	64.70	0.31
14	0.2	0.1	325	0.5	63.2	63.27	-0.18
15	0.2	0.1	325	6	65.9	66.05	-0.22
16	0.2	0.1	325	14	69.0	68.96	0.01
17	0.2	0.1	325	24	64.7	64.52	0.28
18	0.2	0.2	325	0.125	61.6	63.37	-2.87
19	0.2	0.2	325	2	66.0	65.86	0.21
20	0.2	0.2	325	8	69.9	68.40	2.15
21	0.2	0.2	325	16	70.9	69.01	2.66
22	0.2	0.2	325	32	64.8	63.14	2.56
23	0.2	0.4	325	2	64.9	65.58	-1.04
24	0.2	0.4	325	10	71.5	70.00	2.07
25	0.2	0.4	325	20	67.4	68.07	-1.00
26	0.2	0.4	325	32	64.2	64.61	-0.64

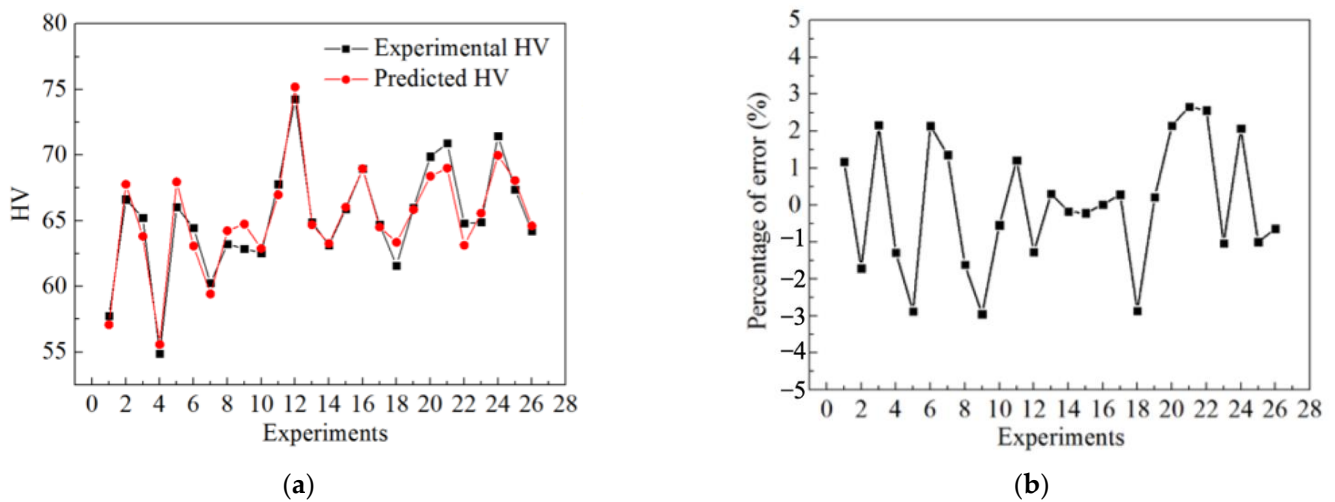


Figure 7. (a) Comparison of experimental and predicted results for HV; (b) percentage of error.

3.2. Regression Model Results

HV is expressed as a polynomial function of the input variables in coded form. The regression model is derived from the experimental results, as shown in the following formula:

$$HV = 65.174 + 0.304x_1 + 0.626x_2 - 1.409x_3 - 0.167x_4 - 0.497x_1 \times x_4 - 0.418x_3 \times x_4 - 1.837x_3^2 - 6.139x_4^2 \quad (8)$$

where x_i ($i = 1, 2, 3, 4$) is the coded input variable. In addition, the coefficients of the terms suggest the effect of input variables on the *HV*. The coefficient of determination (R^2) is used to test the fit of the regression model. In this study, the value of R^2 is 0.754, indicating that 75.4% of the variability in the *HV* can be explained by the regression model. Furthermore, significance tests are conducted to examine the effect and contributions of input variables and the interaction terms on the response *HV*. If the calculated F ratio exceeds the critical $F_{1-\alpha, k-1, n-k}$ value with degrees of freedom ($k - 1$) and ($n - k$), the terms are significant at the α level of significance ($\alpha = 0.05$, k is the number of terms and n is the number of the experimental dataset). The calculated F value is 11.689, which is greater than the critical $F_{0.95, 8, 68}$ value with degrees of freedom 8 and 68, meaning that the model is statistically significant at the 0.05 level of significance. Therefore, from Equation (8), we can see that the regression model is capable of making accurate predictions. The developed model quantifies the effects of alloying elements and the ageing process on microhardness.

3.3. Model Validation

Table 5 shows the comparison between the model predictions and experimental results, indicating that the predicted results obtained by the BP model and the regression model are well in accordance with the experimental results. As a result, the BP neural network and the regression model are able to make accurate predictions of the mechanical properties of heat-treated Mg-4.2Zn-1.7RE-0.8Zr- x Ca- y Sr alloys.

Table 5. The comparison between the developed models and experimental results.

Inputs				The Response HV		
Ca Content, wt.%	Sr Content, wt.%	Ageing Temperature, °C	Ageing Time, h	Regression Model	BP Model	Experimental Result
0.2	0.4	312.5	16	70.35	67.49	68.91

4. Conclusions

Mg-4.2Zn-1.7RE-0.8Zr alloys with different levels of Ca and Sr content, ageing temperatures and ageing times were successfully fabricated. The influential variables and responses were systematically investigated. The conclusions are as follows:

- (1) The ANN model was established using the BP algorithm. The architecture (4-8-1) was in good agreement with that of the experimental values with a correlation coefficient above 0.95.
- (2) The regression model was adopted to model the mechanical properties of the heat-treated experimental alloys. The adequacy of the models was tested by the coefficient of determination and Fisher's criterion. The nonlinear regression model was statistically adequate.
- (3) Predicted results obtained by the BP model and the regression model are well in accordance with experimental results, indicating developed models can reliably predict the mechanical properties of heat-treated Mg-4.2Zn-1.7RE-0.8Zr- x Ca- y Sr alloys. Therefore, time-consuming experiments can be reduced and, hence, considerable savings in terms of cost and time could be obtained by using the developed BP model and the regression model.

Author Contributions: Methodology, Y.F.; software, Z.S. and Y.F.; validation, C.L.; formal analysis, Y.W.; writing—original draft preparation, Y.F.; writing—review and editing, Y.X.; supervision, X.Z.; project administration, Y.F.; funding acquisition, C.L. All authors have read and agreed to the published version of the manuscript.

Funding: This work was financially supported by the Major Special Projects of the Plan “Science and Technology Innovation 2025” (No. 2019B10105, 2019B10086, 2019B10103, 2020Z096, 2020Z060) and the Ningbo Natural Science Foundation (No. 202003N4340).

Institutional Review Board Statement: Not applicable.

Informed Consent Statement: Not applicable.

Data Availability Statement: Not applicable.

Conflicts of Interest: The authors declare no conflict of interest.

Appendix A

Table A1. The experimental results.

No.	Inputs				Output
	X ₁ : Ca Content, wt.%	X ₂ : Sr Content, wt.%	X ₃ : Ageing Temperature, °C	X ₄ : Ageing Time, h	Y: HV
1	0	0	300	0.125	54.9
2	0	0	300	0.5	61.1
3	0	0	300	1	64.2
4	0	0	300	2	65.9
5	0	0	300	6	66.5
6	0	0	300	8	66.2
7	0	0	300	10	67.6
8	0	0	300	12	66.6
9	0	0	300	16	65.1
10	0	0	300	20	65.2
11	0	0	300	32	65.5
12	0	0	325	0.25	58.4
13	0	0	325	0.5	61.7
14	0	0	325	1	63.1
15	0	0	325	2	64.7
16	0	0	325	4	66.7

Table A1. Cont.

No.	Inputs				Output
	X ₁ : Ca Content, wt.%	X ₂ : Sr Content, wt.%	X ₃ : Ageing Temperature, °C	X ₄ : Ageing Time, h	Y: HV
17	0	0	325	6	68.4
18	0	0	325	8	68.7
19	0	0	325	10	69.2
20	0	0	325	14	65.8
21	0	0	325	16	65.9
22	0	0	325	20	65.5
23	0	0	325	28	62.7
24	0	0	325	32	64.4
25	0	0	350	0.125	54.9
26	0	0	350	0.25	57.4
27	0	0	350	1	62.8
28	0	0	350	2	64.0
29	0	0	350	4	62.6
30	0	0	350	8	64.3
31	0	0	350	10	63.3
32	0	0	350	12	62.6
33	0	0	350	20	62.9
34	0	0	350	24	62.1
35	0	0	350	32	61.7
36	0.2	0	325	0.125	59.1
37	0.2	0	325	0.5	61.2
38	0.2	0	325	2	64.5
39	0.2	0	325	4	66.2
40	0.2	0	325	8	67.5
41	0.2	0	325	10	72.8
42	0.2	0	325	14	68.5
43	0.2	0	325	16	66.1
44	0.2	0	325	20	65.4
45	0.2	0	325	28	64.4
46	0.2	0	325	32	63.5
47	0.2	0.1	325	0.125	61.0
48	0.2	0.1	325	1	64.0
49	0.2	0.1	325	2	65.5
50	0.2	0.1	325	4	65.4
51	0.2	0.1	325	8	68.3
52	0.2	0.1	325	10	72.8
53	0.2	0.1	325	12	75.5
54	0.2	0.1	325	16	65.1
55	0.2	0.1	325	20	65.1
56	0.2	0.1	325	28	64
57	0.2	0.1	325	32	63.8
58	0.2	0.2	325	0.5	64.3
59	0.2	0.2	325	1	65.0
60	0.2	0.2	325	4	66.3
61	0.2	0.2	325	6	67.5
62	0.2	0.2	325	10	72.3
63	0.2	0.2	325	12	77.1
64	0.2	0.2	325	14	72.9
65	0.2	0.2	325	20	66.3
66	0.2	0.2	325	24	65.6
67	0.2	0.2	325	28	65.1
68	0.2	0.4	325	0.13	61.5
69	0.2	0.4	325	0.5	64.2
70	0.2	0.4	325	1	65.4
71	0.2	0.4	325	4	65.3
72	0.2	0.4	325	6	66.9

Table A1. Cont.

No.	Inputs				Output
	X ₁ : Ca Content, wt.%	X ₂ : Sr Content, wt.%	X ₃ : Ageing Temperature, °C	X ₄ : Ageing Time, h	Y: HV
73	0.2	0.4	325	8	68.2
74	0.2	0.4	325	12	73.7
75	0.2	0.4	325	14	70.4
76	0.2	0.4	325	16	69.8
77	0.2	0.4	325	24	66.4

References

- Fang, X.G.; Lü, S.L.; Zhao, L.; Wang, J.; Liu, L.F.; Wu, S. Microstructure and mechanical properties of a novel Mg-RE-Zn-Y alloy fabricated by rheo-squeeze casting. *Mater. Des.* **2016**, *94*, 353–359. [[CrossRef](#)]
- Pan, H.; Kang, R.; Li, J.; Xie, H.; Zeng, Z.; Huang, Q.; Yang, C.; Ren, Y.; Qin, G. Mechanistic investigation of a low-alloy Mg-Ca-based extrusion alloy with high strength–ductility synergy. *Acta Mater.* **2020**, *186*, 278–290. [[CrossRef](#)]
- Li, D.; Xue, H.-S.; Yang, G.; Zhang, D.-F. Microstructure and mechanical properties of Mg–6Zn–0.5Y magnesium alloy prepared with ultrasonic treatment. *Rare Met.* **2017**, *36*, 622–626. [[CrossRef](#)]
- Wang, Y.D.; Wu, G.H.; Liu, W.C.; Pang, S.; Zhang, Y. Effects of chemical composition on the microstructure and mechanical properties of gravity cast Mg-xZn-yRE-Zr alloy. *Mater. Sci. Eng. A* **2014**, *594*, 52. [[CrossRef](#)]
- Zhao, M.-C.; Liu, M.; Song, G.-L.; Atrons, A. Influence of Microstructure on Corrosion of As-cast ZE41. *Adv. Eng. Mater.* **2008**, *10*, 104–111. [[CrossRef](#)]
- Neil, W.; Forsyth, M.; Howlett, P.; Hutchinson, C.; Hinton, B. Corrosion of magnesium alloy ZE41—The role of microstructural features. *Corros. Sci.* **2009**, *51*, 387–394. [[CrossRef](#)]
- Fu, Y.; Wang, H.; Zhang, C.; Hao, H. Effects of minor Sr additions on the as-cast microstructure, fluidity and mechanical properties of Mg-4.2Zn-1.7RE-0.8Zr-0.2Ca (wt%) alloy. *Mater. Sci. Eng. A* **2018**, *723*, 118–125. [[CrossRef](#)]
- Wen, K.; Du, W.B.; Liu, K.; Wang, Z.H.; Li, S.B. Microstructures and mechanical properties of homogenization and isothermal aging Mg-Gd-Er-Zn-Zr alloy. *Rare Met.* **2016**, *35*, 443. [[CrossRef](#)]
- Jana, A.; Das, M.; Balla, V.K. Effect of heat treatment on microstructure, mechanical, corrosion and biocompatibility of Mg-Zn-Zr-Gd-Nd alloy. *J. Alloys Compd.* **2020**, *821*, 153462. [[CrossRef](#)]
- Wang, Y.D.; Wu, G.H.; Liu, W.C.; Pang, S.; Zhang, Y.; Ding, W.J. Influence of heat treatment on microstructure and mechanical properties gravity cast Mg-4.2Zn-1.5RE-0.7Zr magnesium alloy. *Trans. Nonferrous Met. Soc. China* **2013**, *23*, 3611–3620. [[CrossRef](#)]
- Zhao, J.W.; Ding, H.; Zhao, W.J.; Huang, M.L.; Wei, D.B.; Jiang, Z.Y. Modelling of the hot deformation behavior of a titanium alloy using constitutive equations and artificial neural network. *Comput. Mater. Sci.* **2014**, *92*, 47. [[CrossRef](#)]
- Sun, Y.; Zeng, W.; Han, Y.; Ma, X.; Zhao, Y.; Guo, P.; Wang, G.; Dargusch, M. Determination of the influence of processing parameters on the mechanical properties of the Ti–6Al–4V alloy using an artificial neural network. *Comput. Mater. Sci.* **2012**, *60*, 239–244. [[CrossRef](#)]
- Liu, Z.; Wang, W.-D.; Gao, W. Prediction of the mechanical properties of hot-rolled C[#]Mn steels using artificial neural networks. *J. Mater. Process. Technol.* **1996**, *57*, 332–336. [[CrossRef](#)]
- Chen, F.F.; Breedon, M.; White, P.; Chu, C.; Mallick, D.; Thomas, S.; Sapper, E.; Cole, I. Correlation between molecular features and electrochemical properties using an artificial neural network. *Mater. Des.* **2016**, *112*, 410–418. [[CrossRef](#)]
- Yang, X.-W.; Zhu, J.-C.; Nong, Z.-S.; He, D.; Lai, Z.-H.; Liu, Y.; Liu, F.-W. Prediction of mechanical properties of A357 alloy using artificial neural network. *Trans. Nonferrous Met. Soc. China* **2013**, *23*, 788–795. [[CrossRef](#)]
- Conduit, B.D.; Jones, N.G.; Stone, H.J.; Conduit, G.J. Design of a nickel-base superalloy using a neural network. *Mater. Des.* **2017**, *131*, 358–365. [[CrossRef](#)]
- Malinov, S.; Sha, W.; McKeown, J. Modelling the correlation between processing parameters and properties in titanium alloys using artificial neural network. *Comput. Mater. Sci.* **2001**, *21*, 375–394. [[CrossRef](#)]
- Malinov, S.; Sha, W. Application of artificial neural networks for modelling correlations in titanium alloys. *Mater. Sci. Eng. A* **2004**, *365*, 202–211. [[CrossRef](#)]
- Manjunath Patel, G.C.; Mathew, R.; Krishna, P.; Parappagoudar, M.B. Investigation of squeeze cast process parameters effects on secondary dendrite arm spacing using statistical regression and artificial neural network models. *Procedia Technol.* **2014**, *14*, 149. [[CrossRef](#)]
- Bhatt, A.; Parappagoudar, M.B. Modeling and Analysis of Mechanical Properties in Structural Steel-DOE Approach. *Arch. Foundry Eng.* **2015**, *15*, 5–12. [[CrossRef](#)]
- Chen, L.; Zhao, Y.; Wen, Z.; Tian, J.; Hou, H. Modelling and Optimization for Heat Treatment of Al-Si-Mg Alloy Prepared by Indirect Squeeze Casting Based on Response Surface Methodology. *Mater. Res.* **2017**, *20*, 1274–1281. [[CrossRef](#)]
- Ozerdem, M.S.; Kolukisa, S. Artificial neural network approach to predict the mechanical properties of Cu-Sn-Pb-Zn-Ni cast alloys. *Mater. Des.* **2009**, *30*, 764. [[CrossRef](#)]

-
23. Soundararajan, R.; Ramesh, A.; Sivasankaran, S.; Sathishkumar, A. Modeling and Analysis of Mechanical Properties of Aluminium Alloy (A413) Processed through Squeeze Casting Route Using Artificial Neural Network Model and Statistical Technique. *Adv. Mater. Sci. Eng.* **2015**, *2015*, 714762. [[CrossRef](#)]
 24. Li, J.-C.; Zhao, D.-L.; Ge, B.-F.; Yang, K.-W.; Chen, Y.-W. A link prediction method for heterogeneous networks based on BP neural network. *Phys. A Stat. Mech. Appl.* **2018**, *495*, 1–17. [[CrossRef](#)]